International Journal of Mechanical, Industrial and Aerospace Sciences
ISSN: 2517-9950
Vol:6, No:8, 2012

An Experimental Helicopter Wind Envelope for Ship Operations

R. Bardera Mora

***Abstract*—**Launch and recovery helicopter wind envelope for a ship type was determined as the first step to the helicopter qualification program. Flight deck velocities data were obtained by means of a two components laser Doppler anemometer testing a $1/50^{th}$ model in the wind tunnel stream. Full-scale flight deck measurements were obtained on board the ship using a sonic anemometer. Wind tunnel and full-scale measurements were compared, showing good agreement and finally, a preliminary launch and recovery helicopter wind envelope for this specific ship was built.

***Keywords*—**Flight deck flow, relative wind, ship airwake, wind envelope

I. Introduction

AERODINAMIC environment in the vecinity of a ship is highly complex and influenced by a large number of factors. Land-based helicopter operations are typically carried out over large flat platforms in open spaces under low airwake turbulence levels. The ship superstructure produces high airwake turbulence levels and the platform is never static. The interaction of the atmospheric wind and sea state with the ship creates the operational environment for the helicopter, different for every ship type [1]. Shipboard helicopter operations are performed in a very adverse and turbulent environment. Relative wind over the flight deck may be constrained by ship operational requirements, forcing the aircraft to land in non-ideal conditions [1]. Operations on board ships require special procedures which introduce additional limitations. These limitations are not provided by the helicopter manufacturer, since they depend to a large extent on the ship involved and its environment [2].Airflow characteristics above the ship's flight deck and along the flight approach paths are usually measured on a scaled model in the wind tunnel and verified experimentally on the actual subject ship. A preliminary flight envelope is assessed by determining the influence of the ship environment on the helicopter capabilities. Finally the preliminary envelope
is verified by means of flight trials on the ship. The test results lead to safe maximum Ship Helicopter Operational Limitations (SHOLs) [2]. Wind limitations are a key piece in the helicopter-ship qualification testing program. The wind limitations data are presented in graph form as a polar diagram (launch/recovery wind envelope), the radius representing the wind speed and the azimuth the wind direction as measured by the ship's systems.

R. Bardera Mora is with the Experimental Aerodynamics Branch of the National Institute of Aerospace Technology, Ctra. Ajalvir, p.k., 4, Madrid, SPAIN (phone: 34 915201637; fax: 34 915202033; e-mail: barderar@ inta.es).

All launch and recovery operations sequences need to establish a steady hover 5 meters (~ 15 feet) above the flight deck before descending vertically and landing [1]. This point is located vertically on the half deck length and width [3] and represents a very hazardous path point because the helicopter is hovering into the superstructure airwake. This paper presents the results obtained when measuring the flow velocity in the critical point of flight deck. The measures were carried out both in wind tunnel and on board full-scale ship and compared by means of graphs and regression analysis.Finally, a preliminary launch/recovery wind envelope for a specific ship was built from wind tunnel data as a first step to the ship-helicopter qualification program. Thus subsequent steps of the program are dedicated to complete additional information about flight tests on board by means of helicopter and ship key parameters.

II. Relative Wind

An axes body system fixed to the ship (referred to as the ship coordinate system) is defined in order to perform a wind velocities study [4]. The origin of the ship coordinate system is located in the plane of the ship waterline, at the mid point of the for-aft line of symmetry. Assuming a ship rectilinear cruise at constant velocity $\boldsymbol{V_S}$, rectilinear cruise along the x axis and the atmospheric wind is blowing over the ship with velocity $\boldsymbol{V_W}$ after β angle with the *x* axis (see Fig. 1).
The $\boldsymbol{V_S}$ and $\boldsymbol{V_W}$ vector velocities are coplanar and parallel to the sea plane.

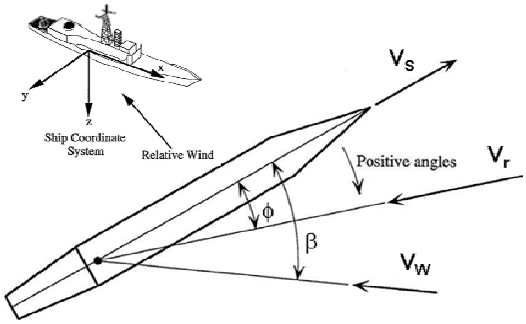

Fig.1. Coordinate system and velocities [4]

The relative wind velocity ***Vr*** is the wind vector resulting from the true wind (atmospheric wind) and ship's course and speed, and is given by,

$$\boldsymbol{V_r} = \boldsymbol{V_W} - \boldsymbol{V_S} \quad (1)$$

$$\boldsymbol{V_r} = V_r\,(-\cos\phi\cdot\boldsymbol{i} - \sin\phi\cdot\boldsymbol{j}) \tag{2}$$

where ***i, j*** are unitary vectors along the *x* and *y* axes, respectively, and ϕ is the relative wind angle between relative wind and the longitudinal ship axis (Fig. 2).
The relative wind vector components are obtained by projection over the ship coordinate system, $u = \boldsymbol{Vr}\cdot\boldsymbol{i}$ and $v = \boldsymbol{Vr}\cdot\boldsymbol{j}$ giving,

$$\begin{Bmatrix} u \\ v \end{Bmatrix} = \begin{Bmatrix} -V_r\cdot\cos\phi \\ -V_r\cdot\sin\phi \end{Bmatrix} \tag{3}$$

Moreover, these components could be as a β angle function, giving,

$$\begin{Bmatrix} u \\ v \end{Bmatrix} = \begin{Bmatrix} -V_W\cdot\cos\beta - V_S \\ -V_W\cdot\sin\beta \end{Bmatrix} \tag{4}$$

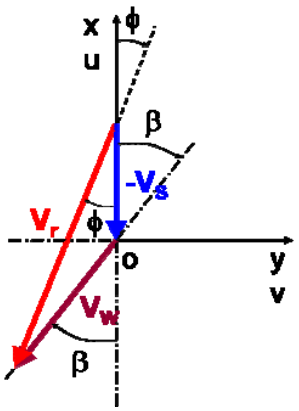

Fig. 2 Wind velocities diagram

The angles are related to wind velocities as follows,

$$\frac{\sin\phi}{\sin\beta} = \frac{V_W}{V_r} \tag{5}$$

The relative wind velocity modulus is given by,

$$V_r = \sqrt{V_W^2 + V_S^2 + 2V_W V_S\cos\beta} \tag{6}$$

The tangent of the relative wind angle is given by,

$$\tan\phi = \frac{V_W\cdot\sin\beta}{V_W\cdot\cos\beta + V_S} \tag{7}$$

III. Flight Deck Flowfield

The flight deck is the ship helideck area located downstream the hangar. One of the largest factors in the variation of flight deck wind flow is the ship or landing platform structure which is by definition a bluff body [5].

Bluff bodies are defined as having a massive separated region in its wake at Reynolds number ranges of order 10^4 and greater [5].

Two dimensional flight deck flowfield approximates to that of a backwards facing step (Fig. 3), with a closed recirculation zone bounded by an unsteady shear layer emanating from the top of the hangar and reattaching on the flight deck [3].

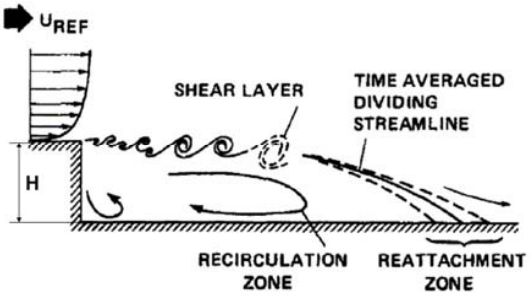

Fig. 3 Two dimensional flight deck flowfield [3]

Extending the model into three dimensions requires to consider the flow perpendicular to the vertical face. Literature [6]-[8] suggests a characteristic flow as shown in Fig. 4 which has been observed through extensive flow visualization tests. A large recirculation region behind the step is produced by the flow incoming to the flight deck from the sides of the ship and causing counter-rotating vortices on each side of the recirculation region. The results in a unsteady horseshoe vortex structure. This unsteadiness of the flow causes this structure to grow, dissipate and move spatially in a unpredictable manner. Adding another degree of complexity, situations where the freestream has a crosswind component must also be considered [9].

A bluff body immersed in a fluid stream will shed vortices with the called natural shedding frequency *f*,

$$f = \frac{U\cdot St}{L} \tag{8}$$

where *U* is the free stream velocity, *L* is a characteristic body dimension (usually width) and *St* is the Strouhal number for shedding, which is in general a function of the body shape and the Reynolds number.

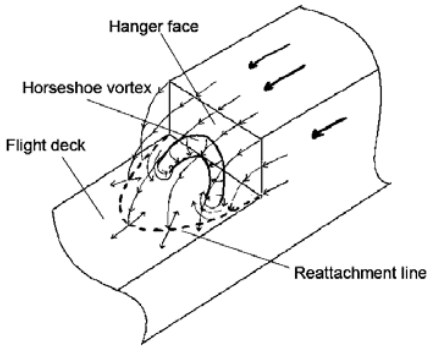

Fig. 4 Three dimensional flight deck flowfield [9]

Reynolds number *(Re)* that represents the inertial to viscous forces ratio is given by,

$$\mathrm{Re} = \frac{\rho U L}{\mu} \tag{9}$$

where ρ is the fluid density, U the flow velocity, L is a characteristic body dimension and μ the dynamic viscosity coefficient. Thus the typical Reynolds number of the aerodynamic flow around a ship is $Re \sim 10^7$ [10].

Moreover, the aerodynamic flow around a ship is incompressible, so the Mach number is of order $5 \cdot 10^{-2}$. Mach number *(Ma)* representing the flow compressibility is given by,

$$Ma = \frac{U}{a} \tag{10}$$

where a is the local sound velocity.

IV. Wind Tunnel Tests

Wind tunnel tests are based on the physical similarity laws applied to the model and prototype flows.

Physical similarity laws are divided in three types: geometric, kinematic and dynamic.

Geometric similarity requires that all dimensions of the model and prototype have the same length scale ratio,

$$\lambda_L = L_m / L_p \tag{11}$$

where L_m y L_p represents the model and the prototype lengths, respectively.

Kinematic similarity requires that the model and prototype have the same velocity scale ratio at all points [11],

$$\lambda_V = V_m / V_p \tag{12}$$

where V_m y V_p represents the model and the prototype flow velocities, respectively.

Dynamic similarity exists when the model and prototype have the same length, time and force scale ratios. Geometric similarity is a first requirement.

For no free surface and incompressible flow model and prototype Reynolds numbers must be equal $(Re_m = Re_p)$ [12].

If kinematic viscosities are equal (i.e.: prototype and model are both in air under atmospheric conditions), Reynolds number scaling requires simply that the velocity scale ratio is given by [11],

$$\lambda_V = \lambda_L^{-1} \tag{13}$$

Time scale ratio is [12],

$$\lambda_T = \lambda_L / \lambda_V = \lambda_L^2 \tag{14}$$

A. Kinematic Similarity

The velocity scale ratio exists between homologous points, hence, the relative wind V_r over the ship is related to the free stream wind tunnel velocity V_t as follows,

$$\lambda_V = \frac{V_t}{V_r} \tag{15}$$

dividing both velocity scale expresions we obtain,

$$1 = \frac{V_m / V_t}{V_p / V_r} = \frac{\hat{V}_m}{\hat{V}_p} \tag{16}$$

where $\hat{V}_m$ and $\hat{V}_p$ are non-dimensional airflow velocities in the model and prototype, respectively, and finally,

$$\hat{V}_m = \hat{V}_p \tag{17}$$

that indicates non-dimensional airflow velocities in the model and prototype are equal.

B. Dynamic Similarity

For wind tunnel test of bluff bodies like trucks, buildings and ships, it is not necessary Reynolds numbers equality because the flow is Reynolds number independent above some threshold value of Reynolds ($Re_{cr} \sim 10^5$), typically when the boundary layer and the wake are both fully turbulent [13].

Moreover, it has been demonstrated that the flow characteristics for several sharp-edges bodies are unchanged with Re varying from 10^4 y 10^7. Although Reynolds based on full-scale ship beam could be of an order of magnitude larger, it can be argued that no significant changes will occur with this increase in Reynolds [10].

C. Boundary Layer

When testing ships in wind tunnels it is usual to simulate a uniform velocity profile with the minimum of turbulence [5]. That is justified because the roughness length Z_0 depends on the mean wind speed, because growing wind speeds increase the height of the waves and consequently the surface roughness. However, aerodynamically waves turn out to be very smooth, probably because they are rounded, and in general are translating in the mean wind direction [5], [14].

Jensen number *(Je)* is a non-dimensional quantity that determines the characteristic length (L_c) to the roughness length (Z_0) ratio [15],

$$Je = \frac{L_c}{Z_0} \tag{18}$$

When the Jensen number is above some value (typically 2000) the roughness length effect is independent of *Je* and the boundary layer effects are not relevant for the problem solution.

A typical marine surface roughness length $Z_0 \sim 10^{-3}$ meters [16] following equation (18) requires a characteristic length $Lc \sim 2$ m when *Je* is 2000. Typical beam measurements for non-carrier ships (frigates) range from about 14 to 19 m with helideck elevations from 2 to 6 m [5] hence roughness length effect is not relevant for these ship type.

D.Experimental Set-up

A 1/50th scale (λ_L = 1/50) wood model of the above waterline portion of a ship has been built and tested in the wind tunnel (Fig. 5). The model is two meters in length and 0.17 meters in hangar height (H). The hangar width (beam) is 1.65 H.

The wind tunnel is a low-speed continuous-flow type with an elliptic open test section (3 m x 2 m) and closed circuit. The maximum airflow velocity is 60 m/s (450 kW) while the turbulence intensity is 0.8%. Flat floor tests are possible situating a mobile platform in the test section. The flat platform simulates the marine boundary layer when testing ship models.

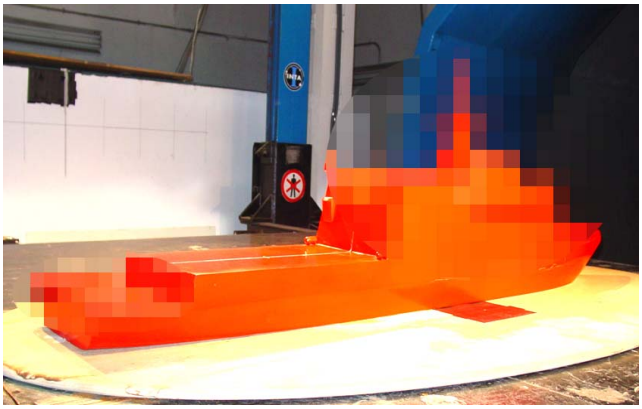

Fig. 5 Ship model on the wind tunnel floor

The wind tunnel freestream was 20 m/s corresponding to a Reynolds number based on the hangar width of 3.9E5, above the critical Reynolds number. Then the vortex shedding frequency into the flight deck flow can be estimate from the Strouhal number (*St* is 0.15 for bluff bodies such as squared or rectangular cylinders, [17]) resulting the vortex shedding frequency of approx. 11 Hz following the equation (8).

Marine boundary layer effects were no simulated because the helideck heigh relative to the wind tunnel floor was 0.125 meters giving a Jensen number of 6250 (> 2000).

Measurement volume was located 0.10 m (0.6H) above the flight deck vertically over the center of the helideck.

The model was positioned to different relative wind angles (each 10 degrees) using an automatic traverse system which is located below the tunnel platform.

Each set of measurements was done three times in order to verify the repetibility.

E. Instrumentation

Laser Doppler Anemometry (LDA) was used to acquire wind velocity data. LDA is a non-intrusive optical measurement technique used to measure the velocity at a point of the flow.

A commercial two components Laser Doppler Anemometer system from TSI, Inc. was used to measure two components of the velocity. Light source is provided by a continuous 3 watts Argon-ion laser mod. INNOVA 70C.

The laser is connected to an optic fiber for illumination and reception of back-scattered light from the tracer particles. Two velocity components were measured simultaneously using two independent chanels, corresponding to different wavelengths: 514.5 nm (green) and 488 nm (blue).

The signal output from the Photo Detector Module (PDM 1000) is sent to the signal processor (FSA 4000) and FlowSizer data analysis software resolves the velocity components.

Olive oil seeding particles 1 μm in diameter were produced by means of a Laskin aerosolgenerator [18]. The particles were injected into the settling chamber six meters upstream the wind tunnel test section.

The position analyzed was above 0.10 m and centered on the model flight deck but varying the incidence angle of the wind, in order to simulate different relative wind angle.

From the laser Doppler anemometer measurements the non-dimensional wind data in the model flight deck are obtained as a relative wind angle function, after the following expressions,

$$\hat{u}_{tunnel} = \frac{u_{lda}}{V_t} \tag{19}$$

$$\hat{v}_{tunnel} = \frac{v_{lda}}{V_t} \tag{20}$$

where u_{lda} and v_{lda} represents the velocity components averaged over five thousand samples measured by the LDA in the critical point over the flight deck and V_t is the modulus of the mean wind tunnel free stream velocity. The velocity data are normalised by the free stream velocity (not the local velocity magnitude) following [3].

Sampling rate of LDA was of order 600 Hz, enough after the Nyquist criteria, because the shedding frequency was estimated around 11 Hz, according to equation (8).

The wind tunnel free stream velocity during the test is known by a differential pressure transducer, the calibration factor of the tunnel, the pressure and temperature of the wind tunnel fluid veine.

V. On board Measurements

Wind velocities measurements above the flight deck obtained from the wind tunnel were verified by tests carried out on board the ship.

The ship course was fixed during 15 minutes. The relative wind angle was incremented by 10 degrees each 15 minutes from -90º to +90º. The mean ship velocity during the experiments was about 4 m/s (~ 8 knots).

A sonic three-components anemometer Metek mod. USA-1 [19] was located in the center of flight deck over a mast 5 meters height. Valid on board measurements requires a correct orientation of the anemometer with the longitudinal axis ship (see Fig. 6). The anemometer orientation was done by means of a mirror and a laser beam.

The non-dimensional wind velocity in the flight deck is obtained from the sonic anemometer measurements after the following expressions,

$$\hat{u}_{ship} = \frac{u_{an}}{\overline{V}_r} \quad (21)$$

$$\hat{v}_{ship} = \frac{v_{an}}{\overline{V}_r} \quad (22)$$

where u_{an} and v_{an} represents the velocity components measured by the sonic anemometer in the critical point over the flight deck and $\overline{V}_r$ is the modulus of the mean relative wind velocity blowing on the ship.

Sampling rate of the sonic anemometer was 1 Hz, hence nine hundred wind data were recorded during fifteen minutes at fixed course (constant relative wind angle).

Sampling frequency was according to the Nyquist criteria because the ship vortex shedding frequency was estimates around 0.1 Hz (St ~ 0.15) according equation (8) based on the hangar width and assuming the relative wind velocity of order 10 m/s.

Fig. 6 Sonic anemometer installed in the flight deck

Environmental conditions were measured by a thermohygrometer Testo 610 and a digital barometer Druck DPI 101.

A second sonic anemometer was installed at the bow of the ship in order to verify the measurements of the ship anemometers. The sonic anemometer was situated on a mast 5 meters above the ship floor and 14 meters upstream the bridge, giving undisturbed relative wind velocities measurements.

Fig. 7 shows the histogram of the relative wind velocity blowing on the bow ship in the configuration to $\phi = 0^o$. During fifteen minutes, nine hundred wind data were recorded in the range from -11.11 to -7.76 m/s. The averaged velocity was -9.41 m/s corresponding to a Reynolds number of 1.3E7 based on the hangar width. Negative velocities indicate the relative flow was coming to the ship. The standard deviation was 0.51 m/s.

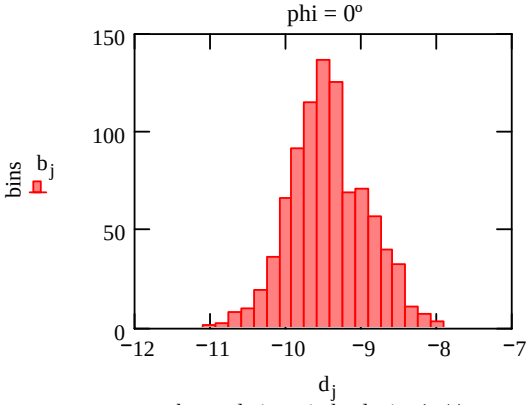

bow relative wind velocity (m/s)

Fig. 7 Histogram of relative wind velocity measured by the bow ship anemometer ($\phi = 0^o$)

Fig. 8 shows u wind velocity component measured by the sonic anemometer located in the flight deck ($\phi = 0^o$). The u wind data were recorded in the range from -5.85 to +0.76 m/s. The u mean velocity was -2.58 m/s and the standard deviation was 1.31 m/s.

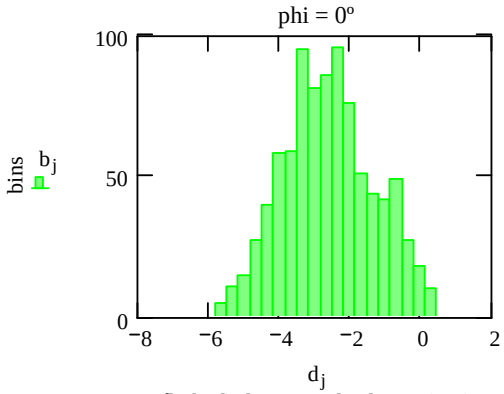

flight deck "u" wind velocity (m/s)

Fig. 8 Histogram of the wind velocity u in the flight deck ($\phi = 0^o$)

Fig. 9 shows v wind velocity component measured by the sonic anemometer located in the flight deck ($\phi = 0^o$). The v wind data were recorded in the range from -4.40 to +4.97 m/s. The v mean velocity was -0.02 m/s and the standard deviation was 1.12 m/s.

The flight deck flow velocity is lower than relative wind velocity blowing on the bow ship. Standard deviation shows the opposite effect; is higher in the flight deck which indicates a higher level of turbulence.

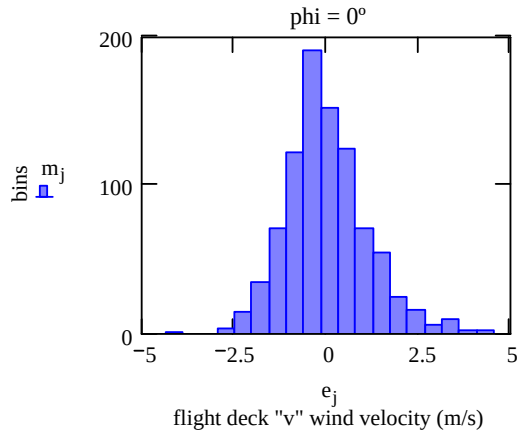

Fig. 9 Histogram of the wind velocity u in the flight deck ($\phi = 0º$).

VI. Results

Results obtained from the wind tunnel model (continuous line) and full-scale on board ship (dots) measurements are showed in graph form (Fig. 10), both curves have a similar trend.

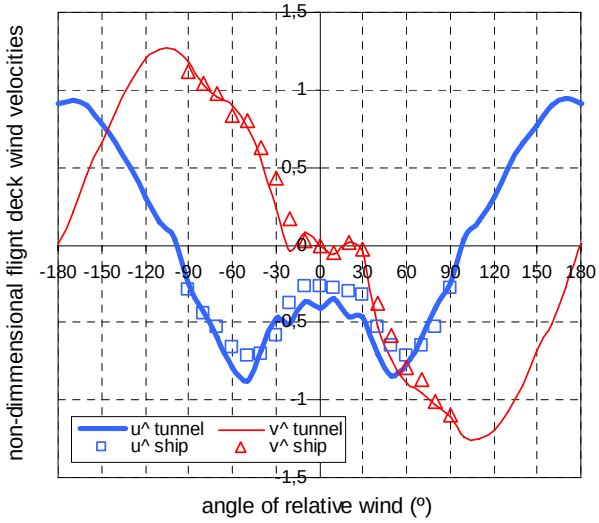

Fig. 10 Non-dimensional wind velocities as a function of relative wind angle

Fig. 11 corresponds to the wind tunnel versus ship data (full-scale) linear regression analysis. The Pearson correlation coefficient (R) was calculated indicating a very high degree of correlation (86% to $\hat{u}$ and 99% to $\hat{v}$).

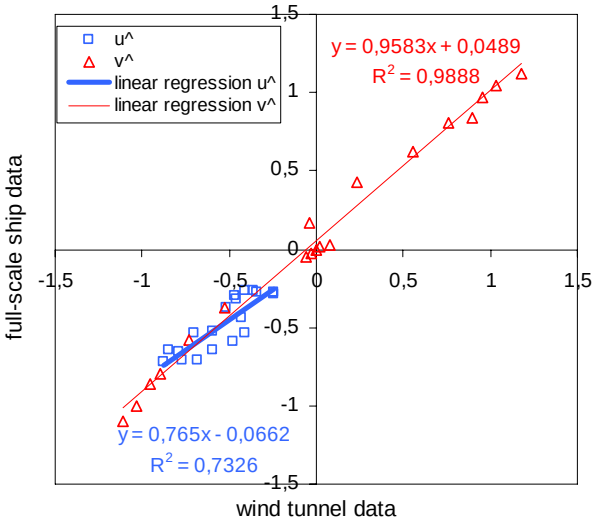

Fig. 11 Regression analysis of wind velocity data.

Turbulence intensity in the flight deck was calculated from wind velocity measurements, both in wind tunnel and in ship, as follows,

$$Iu_{tunnel} = \frac{\sigma u_{lda}}{V_t} \qquad Iv_{tunnel} = \frac{\sigma v_{lda}}{V_t} \tag{23}$$

$$Iu_{ship} = \frac{\sigma u_{ship}}{\overline{V}_r} \qquad Iv_{ship} = \frac{\sigma v_{ship}}{\overline{V}_r} \tag{24}$$

where Ii and σi represent turbulence intensity and standard deviation of the "i" velocity component, respectively. Turbulence intensity is calculated by dividing the standard deviation by the corresponding free stream velocity (not the local velocity magnitude) following [3].

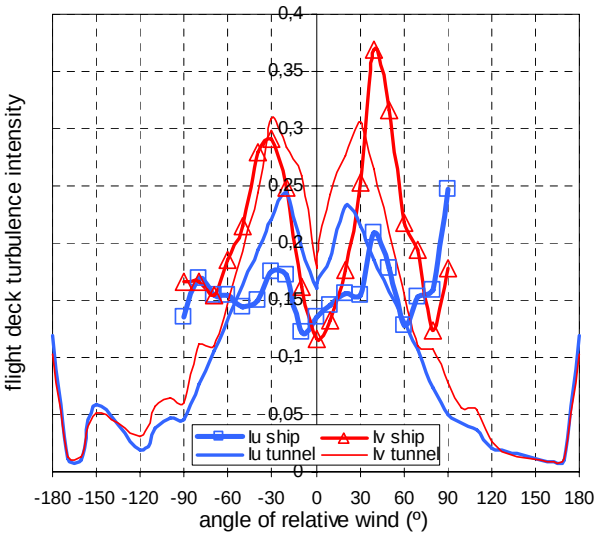

Fig. 12. Turbulence intensity in the flight deck.

Fig. 12 shows the turbulence intensity value for both components obtained from wind velocity measurements. In general wind tunnel and ship curves show similar trend, except some isolated point. Peaks of maximum turbulence intensity are to ϕ = -30º on the negative branch and to ϕ = +30º to +40º on the positive branch. Higher turbulence intensity is approx. 37% as measured in the ship flow for *Iv* turbulence intensity.

Shipboard safety helicopters operations will not exceed aerodynamic limitations which are specific for each helicopter type. Wind velocity limitations could be forward wind velocity 25.0 m/s (~ 50 knots) and sideward wind velocity 17.5 m/s (~ 35 knots) [20],

$$u_{lim} = 25.0\ m/s \tag{25}$$

$$v_{lim} = 17.5\ m/s \tag{26}$$

Criteria above mentioned let us obtain the maximum relative wind velocity based on the non-dimensional velocities measured in the flight deck,

$$Vr_1 = \frac{u_{lím}}{|\hat{u}|} \tag{27}$$

$$Vr_2 = \frac{v_{lím}}{|\hat{v}|} \tag{28}$$

The projection of relative wind on the *x* and *y* axes, let us obtain relative wind velocity in the approach path bounded the outer influence ship flow,

$$Vr_3 = \frac{u_{lím}}{|\cos\phi|} \tag{29}$$

$$Vr_4 = \frac{v_{lím}}{|\sin\phi|} \tag{30}$$

Thus the maximum of the relative wind velocity Vr_{max} for shipboard safety helicopters operations will be determined as the minimum of the possible relative velocities above mentioned,

$$Vr_{\max}(\phi) = \min(Vr_1, Vr_2, Vr_3, Vr_4) \tag{31}$$

Finally, a preliminary launch and recovery helicopter wind envelope for a specific ship was plotted as Fig. 13. The radius representing the relative wind speed and the azimuth the wind direction. The shaded region indicates the wind over deck conditions for safety operations.

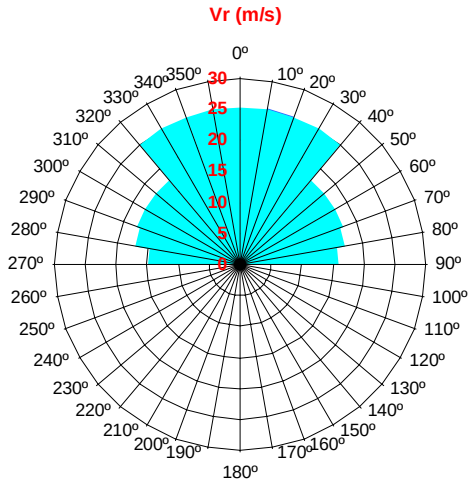

Fig. 13 Launch and recovery helicopter wind envelope diagram (stern approach)

VII. Conclusion

Shipboard helicopter operations are performed in a very adverse environment which introduces operational limitations.

Wind limitations are a key piece in the helicopter-ship qualification testing program. Hence a preliminary flight envelope is assessed by determining the influence of the ship environment on the helicopter capabilities.

In order to investigate a specific ship configuration, a 1/50th scale wood model of a ship has been built and tested in the wind tunnel stream. Laser Doppler Anemometry was used to measure two components of the velocity simultaneously in the critical point of the model flight deck.

Although the wind velocities over the flight deck could be predicted approximately by means of wind tunnel tests, on board the ship measurements must be performed in order to verify wind tunnel tests due to the fact that wind tunnel data are obtained from partial flow simulations mantaining only the relevant parameters of the investigated airflow.

Wind velocities tests on board the ship were carried out by means of a sonic three-components anemometer located on a mast above 5 meters over the flight deck floor in the homologous point tested in the wind tunnel.

Results obtained from wind tunnel were compared to on board measurements by graphs and a linear regression analysis was performed, showing high correlation.

Turbulence intensity in the flight deck was calculated from wind velocity measurement, both, in wind tunnel and in ship and compared, showing similar trend.

Finally, a preliminary launch and recovery helicopter wind envelope for a specific ship was determined from wind tunnel data.

Moreover, in a subsequent step the preliminary wind envelope must be verified by means of flight tests on board the ship acquiring measurements of helicopters and ship key parameters in order to complete the helicopter-ship qualification program [2].

REFERENCES

[1] Geyer, W. P., Long, K. & Carico, D. "Helicopter/Ship Qualification". Part 2: American Clearance Process. *RTO AG-300* Vol. 22/SCI-038. RTO/NATO 2003. ISBN 92-837-1093-2.
[2] Fang, R. & Booij, P. J. A. "Helicopter-Ship Qualification Testing. The Dutch Clearance Process". *National Aerospace Laboratory NLR.* Report no.: NLR-TP-2006-024.
[3] Greenwell, D. I. & Barrett, R. V., "Inclined Screens for Control of Ship Air Wakes", *AIAA 2006-3502*, 3rd AIAA Flow Control Conference 5 - 8 June 2006, San Francisco, California.
[4] Erm, L. P., "A Preliminary Study of the Airwake Model Used in an Existing SH-60B/FFG-7 Helicopter/Ship Simulation Program". DSTO-TR-0015. *Aeronautical and Maritime Research Laboratory*. Australia 1994.
[5] Platt, J. R. "Wind Detection in a Microcosm: Ship/Aircraft Environment Sensors". *IEEE AES Systems Magazine*, February 1998.
[6] Johns, M. K., "Flow Visualization of the Airwake Around a Model of a DD-963 Class destroyer in a Simulated Atmospheric Boundary Layer", *MS Thesis, Naval Postgraduate School, Monterey, CA*, 1988.
[7] Rhoades, M. M., "A Study of the Airwake Aerodynamics Over the Flight Deck of an AOR Model Ship", *MS Thesis, Naval Postgraduate School, CA*, 1990.
[8] Zan, S. J. "Surface Flow Topology for a Simple Frigate Shape", *Canadian Aeronautics and Space Journal*, Vol. 47, No. 1. 2001.
[9] Shafer, D. M., Ghee, T. A. "Active and Passive Flow Control over the Flight Deck of Small Naval Vessels". *AIAA 2005-5265*. 35th AIAA Fluid Dynamics Conference and Exhibit 6-9 June 2005, Toronto, Ontario, Canada.
[10] Lumsden, R. B. "Ship Air-wake Measurement, Prediction, Modelling and Mitigation" DSTL/TR06951. April, 2003. *Defence Science and Technology Laboratory UK.*
[11] Simiu, E. & Scanlan, R. H. "*Wind Effects on Structures. Fundamentals and Applications to Design*". Third Edition. John Wiley & Sons, Inc. 1977.
[12] White, F. "*Fluid Mechanics*". Fourth Edition. McGraw-Hill Companies, Inc. 2002.
[13] Cengel, Y. & Cimbala, J. M., "*Fluid Mechanics: Fundamentals and Applications*". McGraw-Hill, 2006.
[14] Flay R. G. J., "Wind Tunnel Tests on a 1/16th-Scale Laser Model". *University of Southampton. Department of Ship Science. Faculty of Engineering and Applied Science*. June 1992.
[15] Dyrbye, C. & Hansen, S. O. "*Wind Effects on Structures*", John Wiley & Sons, Inc. New York, 1997.
[16] Argyriadis, K. "Recommendations for design of offshore wind turbines External Conditions, state of the art". *Germanischer Lloyd WindEnergie GmbH*. 2003.
[17] Eurocode 1: "*Actions on Structures — General Actions — Part 1-4: Wind Actions*" CEN TC 250. Date: 2004-01. prEN 1991-1-4.
[18] Meyers, J. F., "Generation of particles and seeding". NASA Langley Research Center, USA. Optical Velocity Measurements. Selected Special Topics from previous VKI Lecture series. *Von Karman Institute for Fluid Dynamics*. Belgium. 1994.
[19] METEK USA-1 User Manual. 2005 Metek GmbH-Germany.
[20] Natops Flight Manual Navy Model SH-60B Aircraft. A1-H60BB-NFM-000. May, 2000. *NATEC ELECTRONIC MANUAL*.